

Simulation of optical response functions in molecular junctions

Yi Gao and Michael Galperin

Department of Chemistry and Biochemistry, University of California San Diego, La Jolla, CA 92093, USA

We discuss theoretical approaches to nonlinear optical spectroscopy of molecular junctions. Optical response functions are derived in the form convenient for implementation of Green function techniques, and their expressions in terms of pseudoparticle nonequilibrium Green functions are proposed. The formulation allows to account for both intra-molecular interactions and hybridization of molecular states due to coupling to contacts. Two-dimensional optical spectroscopy in junctions is considered as an example.

I. INTRODUCTION

Interaction of light with matter is an established field of research providing spectroscopic tools for study of interactions and dynamical processes. In molecular systems nonlinear optical spectroscopy is utilized to study transient molecular phenomena [1–8] and local interactions [9, 10], for driving [11] and coherent control [12–14], and for molecular imaging [15, 16]. Theory of nonlinear optical spectroscopy was developed [17, 18] and successfully utilized in numerous studies [19–31].

Rapid development of nanofabrication techniques made possible to study interaction of light with molecular junctions [32–36] leading to appearance of molecular optoelectronics [37]. In molecular junctions electron participate in both optical scattering and quantum transport. Theoretical challenge is description of the two processes on the same footing. *Ab initio* simulations in the field of molecular electronics employ combination of the nonequilibrium Green function (NEGF) method with density functional theory (DFT) [38, 39]. Both NEGF and DFT are formulated in the language of quasiparticles (orbitals); and current through the junction is the primary goal of simulations. Thus it is natural that one of the approaches to describe optical spectroscopy of molecular junctions utilizes quasiparticle language with photon flux giving information on optical response of the system [40–51]. These formulations are capable to account for molecule-contacts coupling exactly, while intra-molecular Interactions are usually treated perturbatively.

Traditional nonlinear optical spectroscopy is formulated in the language of many-body states of isolated molecule (or utilizing dressed states picture) [17, 52], which allows to describe all the intra-molecular interactions exactly. In molecular junctions the formulation is complemented by quantum master equation (QME) to account for current carrying state of the system [53, 54]. Molecular spectroscopy is characterized via response functions obtained from perturbative expansion of photon flux in molecular interaction with radiation field, which requires evaluation of multi-time correlation functions. The latter are usually calculated employing quantum regression theorem [55]. Within the approach interactions with the field define time intervals in which evolution of the system is governed by reduced Liouvillian, while every interaction with optical field also implies

destruction of the molecule-contacts entanglement. The latter is an artifact of the formulation, which (as we show below) may be problematic.

A possible alternative to the QME is utilization of Green function methods of the nonequilibrium atomic limit formulations [56]. These formulations provide consistent way of taking into account molecule-contacts coupling and keep system-bath entanglement intact while the system interact with radiation field. Recently, we utilized the approach to generalize our previous quasiparticle (orbital) based formulations for Raman spectroscopy in molecular junctions [42–45] to account exactly for dependence of molecular normal modes on charging state of the molecule [57]. Here we utilize the nonequilibrium atomic limit tools to complement traditional nonlinear optical spectroscopy formulations [53, 54].

Structure of the paper is the following. After introducing model of molecular junction in Section II we discuss a derivation of optical response functions in form convenient for implementation of Green function techniques (Section II A). Section II B introduces the pseudoparticle nonequilibrium Green functions (PP-NEGF) formulation for the response functions of nonlinear optical spectroscopy. In Section III we specialize our formulation to description of coherent multi-dimensional optical signals in junctions following recent consideration in Ref. [54]. Section IV concludes.

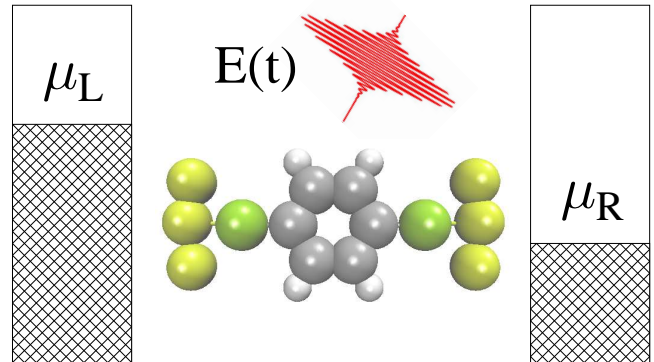


FIG. 1. Sketch of a molecular junction subjected to external radiation field.

II. MODEL

We consider model of a junction consisting of a single molecule M coupled to two metallic contacts L and R and subjected to external radiation field F (see Fig. 1). The contacts are electron reservoirs each at its own equilibrium characterized by electrochemical potentials $\mu_{L,R}$ and temperatures $T_{L,R}$. The field will be treated semi-classically. Following Ref. [17] we derive expression for the optical signal assuming quantum radiation field and transfer to classical description when modeling molecule-field interaction (see details below). In accordance with common practice of molecular spectroscopy formulations below we utilize many-body states $|S\rangle$ of the isolated molecule as a basis. Depending on particular problem these may be electronic or vibronic states of the molecule. We assume that coupling to radiation field is restricted to molecular subspace. Hamiltonian of the model is

$$\hat{H} = \hat{H}_M + \sum_{K=L,R} \left(\hat{H}_K + \hat{V}_{MK} \right) + \hat{H}_F + \hat{V}_{MF} \quad (1)$$

Here \hat{H}_M , \hat{H}_K ($K = L, R$) and \hat{H}_F represent molecule, contacts and radiation field, respectively. \hat{V}_{MK} and \hat{V}_{MF} describe molecular coupling to the contacts and field. Explicit expressions are (here and below $e = \hbar = k_B = 1$)

$$\hat{H}_M = \sum_{S \in M} E_S \hat{X}_{SS} \quad (2)$$

$$\hat{H}_K = \sum_{k \in K} \varepsilon_k \hat{c}_k^\dagger \hat{c}_k \quad (3)$$

$$\hat{V}_{MK} = \sum_{k \in K} \sum_{S_1, S_2 \in M} \left(\hat{V}_{k, S_1 S_2} \hat{c}_k^\dagger \hat{X}_{S_1 S_2} + H.c. \right) \quad (4)$$

$$\hat{H}_F = \sum_{\alpha} \omega_{\alpha} \hat{a}_{\alpha}^{\dagger} \hat{a}_{\alpha} \quad (5)$$

$$\hat{V}_{MF} = - \sum_{\alpha} \sum_{S_1, S_2 \in M} \left(\hat{\mathcal{E}}^{\dagger}(t) \mu_{S_1 S_2} \hat{X}_{S_1 S_2} + H.c. \right) \quad (6)$$

Here \hat{c}_k^\dagger (\hat{c}_k) and \hat{a}_{α}^\dagger (\hat{a}_{α}) create (annihilate) respectively electron in level k of the contact and photon in mode α of the field, $\hat{X}_{S_1 S_2} \equiv |S_1\rangle\langle S_2|$ is the Hubbard operator, and $\mu_{S_1 S_2}$ is matrix element of molecular dipole moment operator. \hat{V}_{MF} is written in the rotating wave approximation and

$$\hat{\mathcal{E}} = \sum_{\alpha} i \left(\frac{2\pi\omega_{\alpha}}{V} \right)^{1/2} \hat{a}_{\alpha} \quad (7)$$

is the positive frequency component of the field written in the long wavelength approximation, which we treat quantum mechanically.

A. Optical response functions

Following Ref. [17] we define optical signal (photon flux) as rate of change of population of the radiation field

modes

$$S(t) \equiv \frac{d}{dt} \sum_{\alpha} \langle \hat{a}_{\alpha}^{\dagger}(t) \hat{a}_{\alpha}(t) \rangle \quad (8)$$

where $\langle \dots \rangle \equiv \text{Tr}[\dots \hat{\rho}]$ indicates quantum and statistical average with density operator $\hat{\rho}$ of the whole system, operators $\hat{a}^{\dagger}(t)$ and $\hat{a}(t)$ are in the Heisenberg picture. Note that the field is treated quantum-mechanically in (8). Utilizing Heisenberg equation of motion one gets for the model (1)-(6)

$$S(t) = -2 \text{Im} \sum_{S_1, S_2} \mu_{S_1 S_2} \langle \hat{\mathcal{E}}^{\dagger}(t) \hat{X}_{S_1 S_2}(t) \rangle \quad (9)$$

Further treatment relies on perturbative expansion of (9) in the molecule-field coupling \hat{V}_{MF} [17]. The expansion is performed on the Keldysh contour [58] to account for nonequilibrium character of the molecular junction. Expressing Eq.(9) in interaction picture and expanding resulting scattering operator in Taylor series leads to

$$S(t) = \sum_{n=0}^{\infty} S^{(2n+1)}(t) \quad (10)$$

where

$$S^{(m)}(t) = -2 \text{Im} \frac{(-i)^m}{m!} \sum_{S_1, S_2} \mu_{S_1 S_2} \int_c d\tau_1 \dots \int_c d\tau_m \langle T_c \hat{\mathcal{E}}^{\dagger}(t) \hat{X}_{S_1 S_2}(t) \hat{V}_{MF}(\tau_1) \dots \hat{V}_{MF}(\tau_m) \rangle_0 \quad (11)$$

Here τ_i ($i = 1, \dots, m$) are contour variables, T_c is the contour ordering operator, operators are in the interaction picture, and subscript 0 indicates evolution under zero-order Hamiltonian $\hat{H}_0 \equiv \hat{H}_M + \sum_{K=L,R} \left(\hat{H}_K + \hat{V}_{MK} \right) + \hat{H}_F$. Note that even contributions in the expansion (10) drop out due to odd number of photon creation/annihilation operators in the correlation function [59]. Substituting explicit expression for \hat{V}_{MF} into (11) leads to explicit expressions. In particular, the first ($m = 1$) and second ($m = 3$) contributions in the expansion (10), which represent respectively linear and third order response, are

$$S^{(1)}(t) = -2 \text{Re} \sum_{\substack{S_1^{(0)}, S_2^{(0)} \\ S_1^{(1)}, S_2^{(1)}}} \mu_{S_1^{(0)} S_2^{(0)}} \mu_{S_1^{(1)} S_2^{(1)}}^* \quad (12)$$

$$\int_c d\tau_1 \langle T_c \hat{\mathcal{E}}^{\dagger}(t) \hat{X}_{S_1^{(0)} S_2^{(0)}}(t) \hat{X}_{S_1^{(1)} S_2^{(1)}}^{\dagger}(\tau_1) \hat{\mathcal{E}}^{\dagger}(\tau_1) \rangle_0$$

$$S^{(3)}(t) = \text{Re} \sum_{\substack{S_1^{(0)}, S_2^{(0)}, S_1^{(1)}, S_2^{(1)} \\ S_1^{(2)}, S_2^{(2)}, S_1^{(3)}, S_2^{(3)}}} \mu_{S_1^{(0)} S_2^{(0)}} \mu_{S_1^{(1)} S_2^{(1)}}^* \quad (13)$$

$$\mu_{S_1^{(2)} S_2^{(2)}} \mu_{S_1^{(3)} S_2^{(3)}}^* \int_c d\tau_1 \int_c d\tau_2 \int_c d\tau_3$$

$$\langle T_c \hat{\mathcal{E}}^{\dagger}(t) \hat{X}_{S_1^{(0)} S_2^{(0)}}(t) \hat{X}_{S_1^{(1)} S_2^{(1)}}^{\dagger}(\tau_1) \hat{\mathcal{E}}^{\dagger}(\tau_1)$$

$$\times \hat{\mathcal{E}}^{\dagger}(\tau_2) \hat{X}_{S_1^{(2)} S_2^{(2)}}(\tau_2) \hat{X}_{S_1^{(3)} S_2^{(3)}}^{\dagger}(\tau_3) \hat{\mathcal{E}}(\tau_3) \rangle_0$$

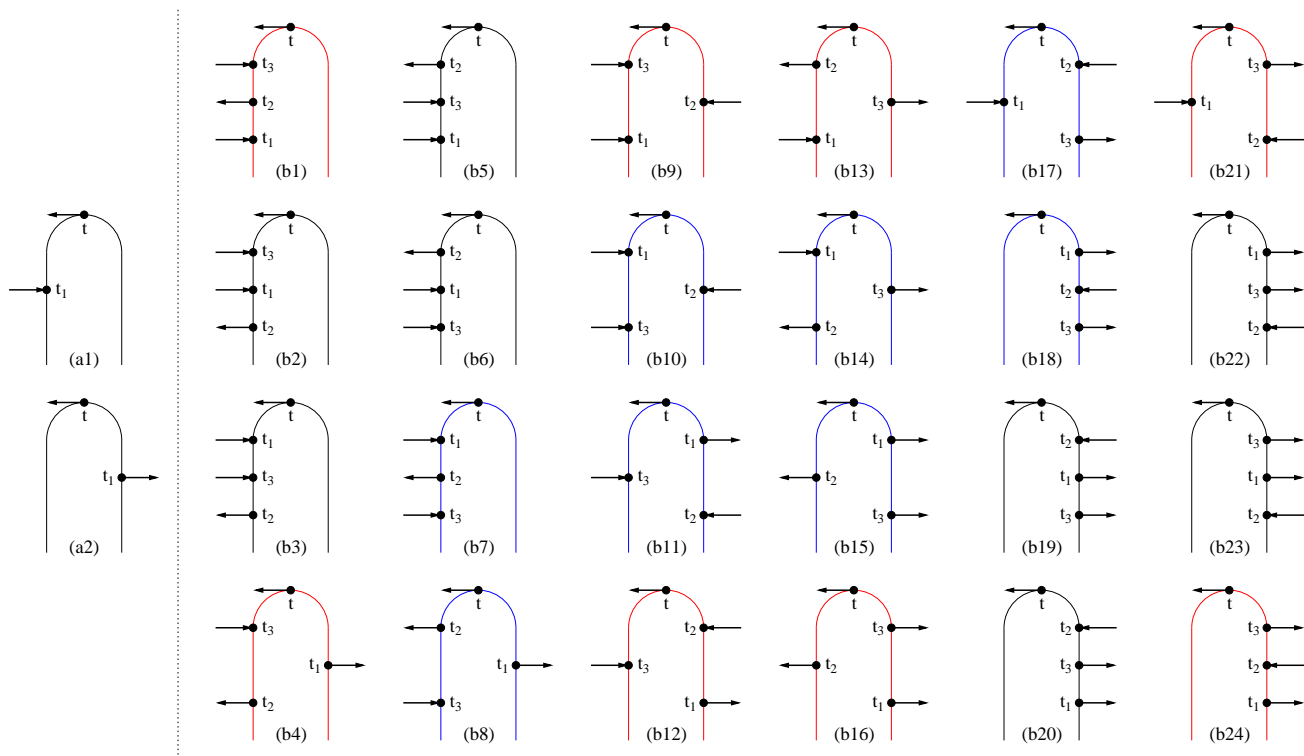


FIG. 2. All possible projections of contour variables τ_i for (a) linear, Eq.(12), and (b) third order, Eq.(13), response functions. t_i are physical times corresponding to contour variables τ_i . Lines pointing to right correspond to positive frequency component of the field, Eq.(14); lines pointing to left indicate their complex conjugate (negative component of the field).

All possible placements (projections) of contour variables τ_i relative to time of the signal t and to each other are shown in Fig. 2a for the linear, Eq.(12), and Fig. 2b for the third order, Eq.(13), response functions. These projections are the double sided Feynman diagrams [17]. Note difference between Hilbert (shown in Fig. 2) and Liouville space projections with the former keeping ordering along the contour while the latter imposing additional restrictions on ordering along the real time axis. As a result number of Liouville space projections is bigger.

Following Ref. [60] at this point we assume that the incoming field is in a coherent state and transfer to classical representation[61]

$$\mathcal{E}(t) = \sum_{\alpha} E_{\alpha}(t) e^{-i\omega_{\alpha}t + i\phi_{\alpha}} \quad (14)$$

where $E_{\alpha}(t)$ is complex time dependent envelope representing, e.g., laser pulse. Thus expression for optical response only requires evaluation of electronic multi-time correlation function.

B. Pseudoparticle formulation

Evaluation of electronic multi-time correlation functions of the type present in Eqs. (11)-(13) is a complicated

problem, which may be approximately treated with a number of techniques. Quantum regression theorem [55] is the usual choice in nonlinear optical spectroscopy [17]. For example, recent works on optical spectroscopy in junctions [53, 54] utilize this approach. Within the approach interactions with the field define time intervals in which evolution of the system is governed by reduced Liouvillian. The approach destroys correlations between molecule and contacts at every instant of interaction with the field. Below we demonstrate that the approximation may be problematic.

We utilize the pseudoparticle nonequilibrium Green function (PP-NEGF) methodology [62–65] as an alternative formulation, which describes molecular system utilizing many-body states, accounts for molecular hybridization due to coupling to contacts, and avoids assumption of molecule-contacts destruction of coherence at times of interaction with radiation field. PP-NEGF has several important advantages: 1. It is conceptually simple; 2. Its practical implementations rely on a set of controlled approximations; 3. Already at the lowest order of the theory, the non-crossing approximation (NCA), it goes beyond usual QME approaches by accounting for both non-Markov effects and hybridization of molecular states; 4. the method is capable of treating the system in the basis of its many-body states. Recently we applied the PP-NEGF to describe results of Raman scattering experiment in the OPV3 molecular junction [57]. Here

we utilize it for a more general description of optical response functions in expansion (10).

PP-NEGF introduces second quantization in the space of many-body states $|S\rangle$ of a system. Pseudoparticle operators \hat{p}_S^\dagger (\hat{p}_S) create (annihilate) state $|S\rangle$

$$\hat{p}_S^\dagger|vac\rangle = |S\rangle \quad (15)$$

where $|vac\rangle$ is vacuum state. Thus Hubbard operators, which appear in the response functions, Eqs. (9), (12) and (13), can be expressed as

$$\hat{X}_{S_1 S_2} \equiv |S_1\rangle\langle S_2| \rightarrow \hat{p}_{S_1}^\dagger \hat{p}_{S_2} \quad (16)$$

The consideration requires extended Hilbert space formulation, physical subspace of which is defined by the normalization condition

$$\sum_S \hat{p}_S^\dagger \hat{p}_S = 1 \quad (17)$$

In the extended Hilbert space the formulation utilizes standard tools of the quantum field theory. Restriction (17) modifies resulting expressions projecting them onto the physical subspace.

Evaluation of multi-time correlation functions is complicated by the non-quadratic character of the molecule-contacts coupling, Eq.(4), in the pseudoparticle representation. Usual perturbative treatment requires expanding correlation functions in the interaction \hat{V}_{MK} up to a particular order, identifying irreducible diagrams, dressing them and formulating corresponding equations-of-motion. Already at the level of linear response, Eq.(12), this will require simultaneous solution of the Dyson and Bethe-Salpeter equations. For simplicity here we rely on a mean-field treatment, where a multi-time correlation function can be approximately presented as a product of pseudoparticle Green functions

$$G_{S_1 S_2}(\tau_1, \tau_2) \equiv -i\langle T_c \hat{p}_{S_1}(\tau_1) \hat{p}_{S_2}^\dagger(\tau_2) \rangle \quad (18)$$

Below we demonstrate that in physically relevant range of parameters the approximation yields reasonable description of optical response.

Keeping in mind that the restriction (17) only allows one lesser pseudoparticle Green function to be present in any diagram [62] after projection (see Fig. 2) we get for an arbitrary correlation function the following approximate expression

$$\langle \hat{p}_1^\dagger(t_1) \hat{p}_2(t_1) \hat{p}_3^\dagger(t_2) \hat{p}_4(t_2) \dots \hat{p}_{2m-1}^\dagger(t_m) \hat{p}_{2m}(t_m) \rangle \approx \quad (19)$$

$$i^m \zeta_1 G_{2m,1}^<(t_m, t_1) G_{23}^>(t_1, t_2) \dots G_{2m-2,2m-1}^>(t_{m-1}, t_m)$$

where $G^<$ ($G^>$) is lesser (greater) projection of the Green function (18) and $\zeta_1 = -1$ (+1) if many-body state 1 is of Fermi (Bose) type [66].

In the extended Hilbert space pseudoparticle Green functions, Eq.(18), satisfy the usual Dyson equation. At

steady state one has to solve equations for retarded and lesser projections [63]

$$\mathbf{G}^r(E) = \left[\mathbf{E}\mathbf{I} - \mathbf{H}_M - \mathbf{\Sigma}^r(E) \right]^{-1} \quad (20)$$

$$\mathbf{G}^<(E) = \mathbf{G}^r(E) \mathbf{\Sigma}^<(E) \mathbf{G}^a(E) \quad (21)$$

Here Green functions \mathbf{G} , molecular Hamiltonian \mathbf{H}_M and self-energies due to molecule-contacts coupling $\mathbf{\Sigma}$ are matrices in the basis of many-body states of an isolated molecule, \mathbf{I} is unity matrix, and $\mathbf{G}^a(E) = [\mathbf{G}^r(E)]^\dagger$ is advanced projection. Each of the expressions (20) and (21) have to be solved self-consistently, since within the formulation self-energies depend on Green functions. The two equations belong to different subspaces and thus should be solved independently: after (20) converges its result (retarded projection of the Green function) is utilized in self-consistent solution of (21). Note that normalization (17) implies the following connection between greater and retarded projections of the Green function [67]

$$\mathbf{G}^>(E) = 2i \text{Im} \mathbf{G}^r(E) \quad (22)$$

For further details and explicit expressions for the self energies see, e.g., Ref. [64].

III. COHERENT 2D SIGNALS

Following consideration in Ref. [54] we now specify to 4-laser pulse sequence for time domain experiment. Radiation field (14) takes the form

$$\mathcal{E}(t) = \sum_{i=1}^4 E_i(t) e^{-i\omega_i t + i\phi_i} \quad (23)$$

where $E_i(t)$ is the complex envelope of i^{th} pulse centered around \bar{t}_i (see Fig. 3). Following Ref. [54] we will be interested in stimulated signal in the fourth order of optical field with phase signature $\phi \equiv \phi_1 - \phi_2 + \phi_3 - \phi_4$.

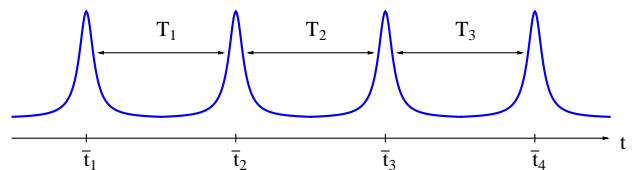


FIG. 3. Laser pulse sequence for time-domain experiment.

The signal is given by 8 projections b1, b4, b9, b12, b13, b16, b21, b24 (and their analogs with $t_1 \leftrightarrow t_3$: b7, b14, b10, b17, b8, b15, b11, b18) of the third order response (13) under restriction $t > t_3 > t_2 > t_1$ (compare

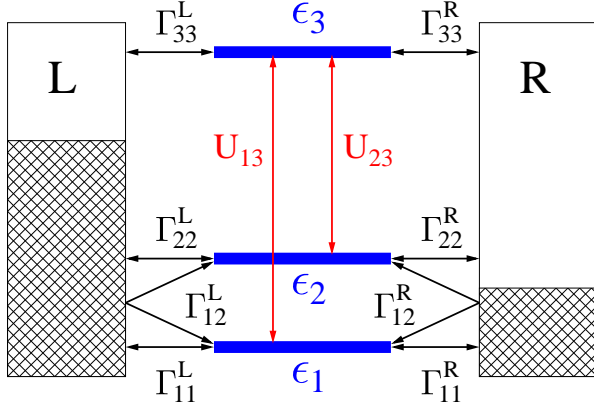


FIG. 4. A model of molecular junction.

with Fig. 2 of Ref. [54]). Explicit expression is

$$S^{(3)}(t) = 2 \text{Re} \sum_{\substack{S_1^{(0)}, S_2^{(0)}, S_1^{(1)}, S_2^{(1)} \\ S_1^{(2)}, S_2^{(2)}, S_1^{(3)}, S_2^{(3)}}} \int_{-\infty}^t dt_3 \int_{-\infty}^{t_3} dt_2 \int_{-\infty}^{t_2} dt_1 \\ \mu_{S_1^{(0)} S_2^{(0)}} \mu_{S_2^{(1)} S_1^{(1)}} \mu_{S_1^{(2)} S_2^{(2)}} \mu_{S_2^{(3)} S_1^{(3)}} \mathcal{E}^*(t) \mathcal{E}(t_3) \mathcal{E}^*(t_2) \mathcal{E}(t_1) \\ \langle [[\hat{p}_{S_1^{(0)}}^\dagger(t) \hat{p}_{S_2^{(0)}}(t); \hat{p}_{S_2^{(3)}}^\dagger(t_3) \hat{p}_{S_1^{(3)}}(t_3)]; \\ \hat{p}_{S_1^{(2)}}^\dagger(t_2) \hat{p}_{S_2^{(2)}}(t_2)]; \hat{p}_{S_2^{(1)}}^\dagger(t_1) \hat{p}_{S_1^{(1)}}(t_1)] \rangle \quad (24)$$

We now introduce the total stimulated signal (see Fig. 3)

$$S_{stim}(T_3, T_2, T_1) \equiv \int_{-\infty}^{+\infty} dt S^{(3)}(t) \quad (25)$$

Assuming short impulses, $E_i(t) \approx E_i \delta(t - \bar{t}_i)$ and utilizing approximation (19) in (24) we get for steady-state transport

$$S_{stim}(\Omega_1, T_2, \Omega_3) \equiv \int_0^\infty dT_3 \int_0^\infty dT_1 e^{i\Omega_3 T_3 + i\Omega_1 T_1} S_{stim}(T_3, T_2, T_1) = 2 \text{Re} \sum_{\substack{S_1^{(0)}, S_2^{(0)}, S_1^{(1)}, S_2^{(1)} \\ S_1^{(2)}, S_2^{(2)}, S_1^{(3)}, S_2^{(3)}}} E_4^* E_3 E_2^* E_1 e^{i\phi} \quad (26) \\ \mu_{S_1^{(0)} S_2^{(0)}} \mu_{S_2^{(1)} S_1^{(1)}} \mu_{S_1^{(2)} S_2^{(2)}} \mu_{S_2^{(3)} S_1^{(3)}} \zeta_{S_1^{(0)}} 2\pi \delta(\omega_1 - \omega_2 + \omega_3 - \omega_4) \int_{-\infty}^{+\infty} \frac{d\epsilon_1}{2\pi} \int_{-\infty}^{+\infty} \frac{d\epsilon_2}{2\pi} e^{iT_2(\omega_1 - \omega_2 + \epsilon_1 - \epsilon_2)} \\ \left(G_{S_1^{(1)} S_1^{(0)}}^<(\epsilon_1) G_{S_2^{(0)} S_2^{(3)}}^>(\epsilon_1 + \Omega_3 + \omega_4) G_{S_1^{(3)} S_1^{(2)}}^>(\epsilon_2) G_{S_2^{(2)} S_2^{(1)}}^>(\epsilon_1 + \Omega_1 + \omega_1) \right. \\ + G_{S_1^{(1)} S_1^{(2)}}^<(\epsilon_2 - \Omega_1 - \omega_1) G_{S_2^{(2)} S_2^{(3)}}^>(\epsilon_1) G_{S_1^{(3)} S_1^{(0)}}^>(\epsilon_2 - \Omega_3 - \omega_4) G_{S_2^{(0)} S_2^{(1)}}^>(\epsilon_2) \\ + G_{S_1^{(3)} S_2^{(1)}}^<(\epsilon_2) G_{S_1^{(1)} S_1^{(2)}}^>(\epsilon_2 - \Omega_1 - \omega_1) G_{S_2^{(2)} S_1^{(0)}}^>(\epsilon_1) G_{S_2^{(0)} S_2^{(3)}}^>(\epsilon_1 + \Omega_3 + \omega_4) \\ + G_{S_2^{(2)} S_2^{(1)}}^<(\epsilon_1 + \Omega_1 + \omega_1) G_{S_1^{(1)} S_2^{(3)}}^>(\epsilon_1) G_{S_1^{(3)} S_1^{(0)}}^>(\epsilon_2 - \Omega_3 - \omega_4) G_{S_2^{(0)} S_1^{(2)}}^>(\epsilon_2) \\ - G_{S_2^{(2)} S_2^{(1)}}^<(\epsilon_1 + \Omega_1 + \omega_1) G_{S_1^{(1)} S_1^{(0)}}^>(\epsilon_1) G_{S_2^{(0)} S_2^{(3)}}^>(\epsilon_1 + \Omega_3 + \omega_4) G_{S_1^{(3)} S_1^{(2)}}^>(\epsilon_2) \\ - G_{S_1^{(1)} S_2^{(3)}}^<(\epsilon_1) G_{S_1^{(3)} S_1^{(0)}}^>(\epsilon_2 - \Omega_3 - \omega_4) G_{S_2^{(0)} S_1^{(2)}}^>(\epsilon_2) G_{S_2^{(2)} S_2^{(1)}}^>(\epsilon_1 + \Omega_1 + \omega_1) \\ - G_{S_1^{(1)} S_1^{(2)}}^<(\epsilon_2 - \Omega_1 - \omega_1) G_{S_2^{(2)} S_1^{(0)}}^>(\epsilon_1) G_{S_2^{(0)} S_2^{(3)}}^>(\epsilon_1 + \Omega_3 + \omega_4) G_{S_1^{(3)} S_2^{(1)}}^>(\epsilon_2) \\ \left. - G_{S_2^{(0)} S_2^{(1)}}^<(\epsilon_2) G_{S_1^{(1)} S_1^{(2)}}^>(\epsilon_2 - \Omega_1 - \omega_1) G_{S_2^{(2)} S_2^{(3)}}^>(\epsilon_1) G_{S_1^{(3)} S_1^{(0)}}^>(\epsilon_2 - \Omega_3 - \omega_4) \right)$$

This result is alternative to Eq.(10) in Ref. [54] theoretical description of 2D optical spectroscopy in junctions. While no experimental result on multi-dimensional optical spectroscopy in junctions have been reported yet, first proposals on utilizing pump-probe approaches for junctions diagnostics were reported recently [68, 69].

Contrary to the usually employed QME based considerations of optical response Eq. (26) avoids assumption of molecule-contacts destruction of coherence at times

of interaction with radiation field. To demonstrate advantage of the formulation we consider a simple model of molecular junction (see Fig. 4) with two low-lying orbitals (e.g., HOMO and HOMO-1) hybridized with states of contacts and (through the contacts) with each other and one higher lying orbital (e.g., LUMO). The model is described by Hamiltonian (1)-(6) with eight many-body

molecular states $\{|S\rangle\}$

$$\begin{aligned} |S_1\rangle &= |0, 0, 0\rangle, \\ |S_2\rangle &= |1, 0, 0\rangle, |S_3\rangle = |0, 1, 0\rangle, |S_4\rangle = |0, 0, 1\rangle, \\ |S_5\rangle &= |0, 1, 1\rangle, |S_6\rangle = |1, 0, 1\rangle, |S_7\rangle = |1, 1, 0\rangle, \\ |S_8\rangle &= |1, 1, 1\rangle \end{aligned} \quad (27)$$

Energies of the states are 0, ε_1 , ε_2 , ε_3 , $\varepsilon_2 + \varepsilon_3$, $\varepsilon_1 + \varepsilon_3$, $\varepsilon_1 + \varepsilon_2$, and $\varepsilon_1 + \varepsilon_2 + \varepsilon_3$, respectively. Quasiparticle representation of the model Hamiltonians for the molecule and its coupling with contacts is

$$\hat{H}_M = \sum_{m=1}^3 \varepsilon_m \hat{d}_m^\dagger \hat{d}_m \quad (28)$$

$$\hat{V}_{MK} = \sum_{k \in K} \sum_{m=1}^3 \left(V_{km} \hat{c}_k^\dagger \hat{d}_m + H.c. \right) \quad (29)$$

Here \hat{d}_m^\dagger (\hat{d}_m) creates (annihilates) electron in orbital m . Hybridization of molecular orbitals with states in the contacts is characterized by dissipation matrix ($K = L, R$)

$$\Gamma_{m_1 m_2}^K(E) = 2\pi \sum_{k \in K} V_{m_1 k} V_{k m_2} \delta(E - \varepsilon_k) \quad (30)$$

which in the wide-band approximation is assumed energy independent. Note that for the model of Fig. 4 we assume contact induced hybridization between orbitals 1 and 2, while orbital 3 does not hybridize with the low lying levels. The model is reasonable, because usual HOMO-LUMO gaps in molecules are at least of the order of 1 eV, which makes hybridization between HOMOs and LUMOs through the contacts negligible.

For the model of Fig. 4 the QME approach will fail to predict stimulated signal (26). From the QME expression for the $S_{stim}(\Omega_1, T_2, \Omega_3)$, Eq. (A1), one sees that coupling (in the absence of the field) between states characterizing optical transition (pair $S_1^{(0)} S_2^{(0)}$ in Eq. (A1); pairs of states ($|S_2\rangle, |S_4\rangle$), ($|S_3\rangle, |S_4\rangle$), ($|S_7\rangle, |S_5\rangle$) and ($|S_7\rangle, |S_6\rangle$) of the model) is necessary for non-zero stimulated signal. In the absence of optical field such coupling can be provided only by contacts, i.e. by dissipation matrix Γ , Eq. (30). As discussed above, for states separated by ~ 1 eV such coupling is negligible. At the same time in the presence of such coupling (for example, for closer lying pairs of states) accurate calculation of the reduced density matrix, which is part of the expression (A1), is required for proper prediction of the signal. At the usual level of consideration (second order in the system-bath coupling) QME is known to fail in this regime [70]. Fig. 5 compares Redfield QME simulations of the reduced density matrix to NEGF results. The latter are exact for the model of Fig. 4. Parameters of the simulations are $T = 300$ K, $\varepsilon_1 = -0.5$ eV, $\varepsilon_2 = -0.2$ eV, $\varepsilon_3 = 0.5$ eV. Fermi energy is taken as origin, $E_F = 0$, and bias is applied symmetrically, $\mu_L = E_F + |e|V_{sd}/2$ and $\mu_R = E_F - |e|V_{sd}/2$. Results of simulations presented

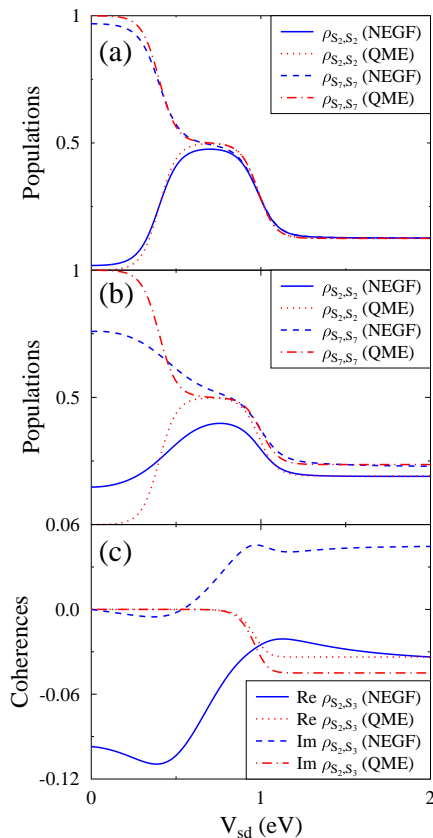


FIG. 5. Reduced density matrix for the model of Fig. 4 vs. applied bias. Redfield QME results are compared to exact NEGF results for (a) weak diagonal and (b) strong non-diagonal molecule-contacts couplings. See text for parameters.

in Fig. 5a employed weak diagonal coupling between molecule and contacts, $\Gamma^K + m_1, m_2 = \delta_{m_1, m_2} 0.01$ eV ($m_{1,2} \in \{1, 2, 3\}$, $K = L, R$). Calculations in Figs. 5b and 5c utilized stronger non-diagonal coupling parameters for levels 1 and 2: $\Gamma_{11}^L = 0.2$ eV, $\Gamma_{11}^R = 0.05$ eV, $\Gamma_{12}^K = \Gamma_{21}^K = \Gamma_{22}^K = 0.1$ eV ($K = L, R$). Fig. 5a shows that for weak diagonal coupling Redfield QME is pretty accurate. However, as shown in Figs. 5b and 5c, in the presence of non-diagonal coupling (this is the situation necessary for simulations of the optical signal within the QME approach) Redfield QME predictions deviate significantly from exact NEGF results (especially in prediction of coherences).

Contrary to the QME approximate PP-NEGF expression, Eq. (26), is capable to reproduce stimulated signal for the model of Fig. 4. Figure 6 compares results of simulations utilizing approximate PP-NEGF expression (26) with exact NEGF results, Eq. (B1). Parameters of the simulations are $\Gamma_{m_1, m_2}^K = 0.05$ eV ($m_{1,2} = 1, 2$, $K = L, R$), $\omega_1 = \omega_4 = 1$ eV, $\omega_2 = \omega_3 = 0.7$ eV. Other parameters are as in Fig. 5. Peak at $\Omega_1 = \Omega_3 = 0$ represents the $1 \rightarrow 3$ transition ($|S_1\rangle \rightarrow |S_4\rangle$ and $|S_7\rangle \rightarrow |S_5\rangle$ in terms of states), $\Omega_1 = \Omega_3 = -0.3$ eV represents tran-

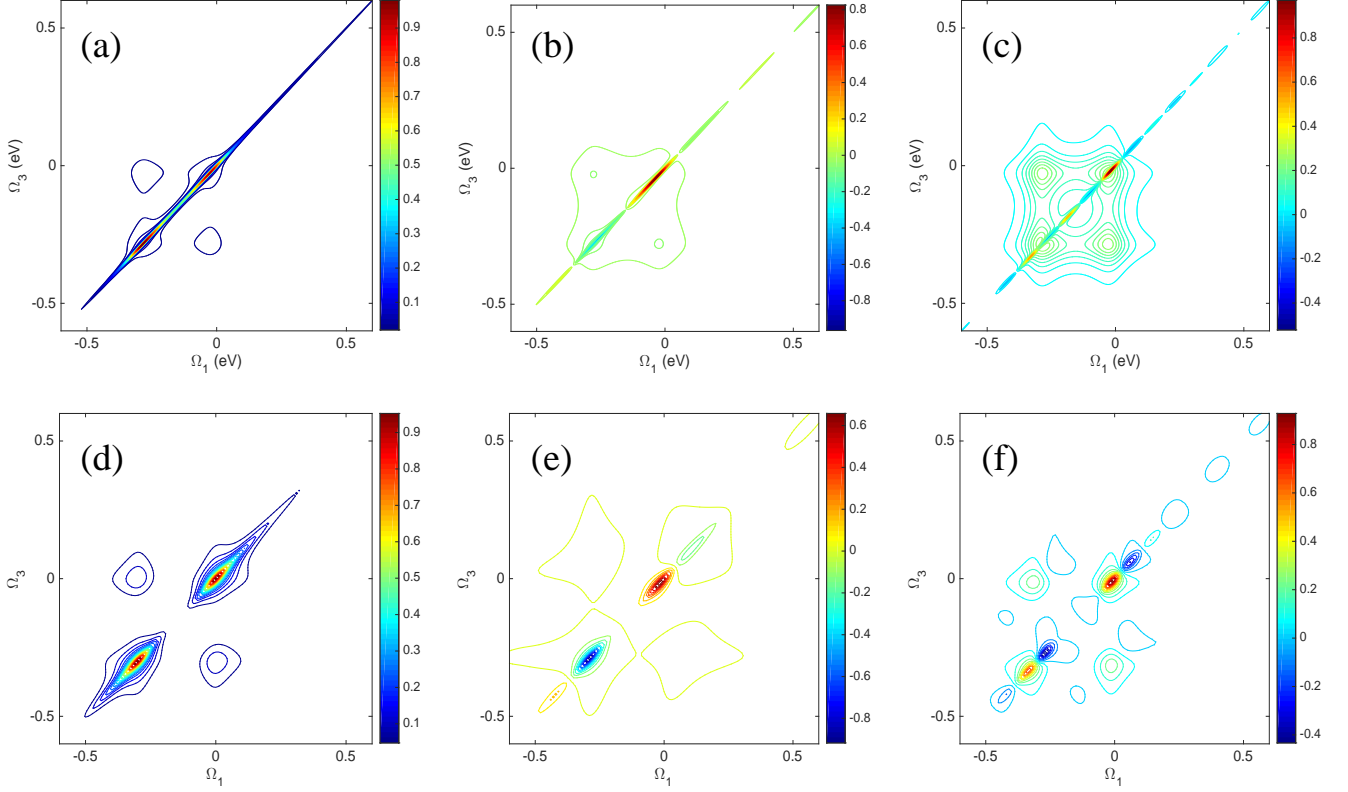


FIG. 6. The stimulated signal $S_{stim}(\Omega_3, T_2, \Omega_1)$ for the model of Fig. 4 at equilibrium, $V_{sd} = 0$. Approximate PP-NEGF results, Eq. (26), are compared with exact NEGF calculations, Eq. (B1). Results for delay times $T_2 = 0, 10$ and 25 fs are shown in panels (a)-(c) for PP-NEGF and (d)-(f) for NEGF. Maximum of the signal is scaled to 1. See text for parameters.

sition $2 \rightarrow 3$ ($|S_3\rangle \rightarrow |S_4\rangle$ and $|S_7\rangle \rightarrow |S_6\rangle$ in terms of states). Off-diagonal peaks ($\Omega_1 = 0, \Omega_3 = -0.3$ eV and $\Omega_1 = -0.3$ eV, $\Omega_3 = 0$) indicate correlation between levels 1 and 3, pairs of states ($|S_2\rangle, |S_3\rangle$) and ($|S_5\rangle, |S_6\rangle$) due to coupling to contacts. One sees that main features of the spectrum are reproduced qualitatively correctly.

Figure 7 shows stimulated signal in a biased junction. Parameters of the simulations are $\Gamma_{11}^L = 0.1$ eV, $\Gamma_{11}^R = \Gamma_{12}^R = \Gamma_{21}^R = 0$. Other parameters are as in Fig. 6. Here level 1 is attached to the left contact only. Also here stimulated signal is reproduced qualitatively correctly by the approximate expression (26). It is interesting to note that under bias the signal can provide information on asymmetry in the junction. At high bias of $V_{sd} = 2$ V levels 2 and 3 have population of $1/2$, while level 1 is fully populated. As a result only transition $1 \rightarrow 3$ is seen in the signal, while electronic transitions in the $2 \rightarrow 3$ channel are compensated by electronic transition in $3 \rightarrow 2$ channel (or hole transitions in $2 \rightarrow 3$). This is easily seen from the structure of Eq. (B1). As a result only one diagonal and one off-diagonal peaks are visible.

IV. CONCLUSION

We consider simulation of optical response functions in molecular junctions. Following standard methodology of the nonlinear optical spectroscopy and restricting consideration to classical radiation fields we first express optical response functions in the form convenient for implementation of Green function techniques, and then propose a simple approximate scheme for representing the response functions in terms of the pseudoparticle nonequilibrium Green functions (PP-NEGF). Similar to more traditional quantum master equation based approach, our formulation is capable to describe optical response in the basis of many-body states of the system. It also accounts approximately for hybridization of molecular states due to coupling to contacts. Finally, it avoids approximation of the standard QME treatment when each instant of interaction with light results in destruction of molecule-contacts entanglement. Within simple 3-level model (e.g., HOMO-1, HOMO and LUMO) and utilizing stimulated signal in the fourth order of optical field we illustrate the advantages of the proposed approximate scheme. Comparing results of the PP-NEGF simulations with exact (for the chosen noninteracting model) NEGF results we show that the formulation reproduces stimu-

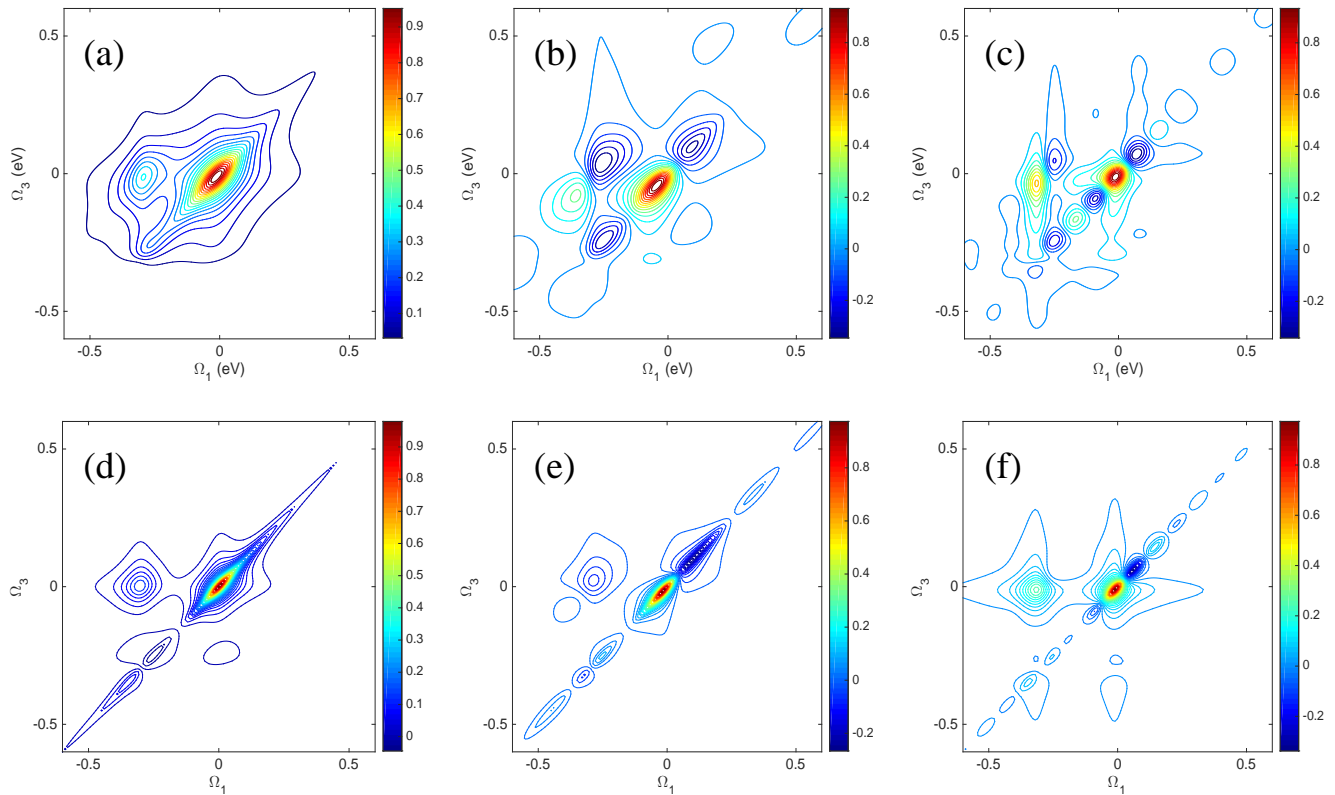


FIG. 7. The stimulated signal $S_{stim}(\Omega_3, T_2, \Omega_1)$ for the model of Fig. 4 in biased junction, $V_{sd} = 2$ V. Approximate PP-NEGF results, Eq. (26), are compared with exact NEGF calculations, Eq. (B1). Results for delay times $T_2 = 0, 10$ and 25 fs are shown in panels (a)-(c) for PP-NEGF and (d)-(f) for NEGF. Maximum of the signal is scaled to 1. See text for parameters.

lated signal qualitatively correctly, when QME based approach fails. Finally, we show that 2d stimulated signal can provide information on asymmetry in junctions.

ACKNOWLEDGMENTS

M.G. gratefully acknowledges support by the US Department of Energy (Early Career Award, de-sc0006422).

Appendix A: QME expression for stimulated signal

Employing quantum regression theorem in evaluation of multi-time correlation functions in Eq.(13) leads to the following expression for stimulated signal at steady-state transport (compare with Eq.(10) of Ref. [54])

$$\begin{aligned}
S_{stim}(\Omega_1, T_2, \Omega_3) &\equiv \int_0^\infty dT_3 \int_0^\infty dT_1 e^{i\Omega_3 T_3 + i\Omega_1 T_1} S_{stim}(T_3, T_2, T_1) \\
&= 2 \text{Im} \sum_{\substack{S_1^{(0)}, S_2^{(0)}, S_1^{(1)}, S_2^{(1)} \\ S_1^{(2)}, S_2^{(2)}, S_1^{(3)}, S_2^{(3)}}} \sum_{S_a, S_b, S_c} E_4^* E_3 E_2^* E_1 e^{iT_2(\omega_1 - \omega_2) + i\phi} \\
&\mu_{S_1^{(0)} S_2^{(0)}} \mu_{S_2^{(1)} S_1^{(1)}} \mu_{S_1^{(2)} S_2^{(2)}} \mu_{S_2^{(3)} S_1^{(3)}} 2\pi \delta(\omega_1 - \omega_2 + \omega_3 - \omega_4) \\
&\left(\mathcal{G}_{S_1^{(0)} S_2^{(0)}, S_c S_2^{(3)}}^r(\Omega_3 + \omega_4) \mathcal{G}_{S_c S_1^{(3)}, S_b S_1^{(2)}}^r(T_2) \mathcal{G}_{S_b S_2^{(2)}, S_a S_2^{(1)}}^r(\Omega_1 + \omega_1) \rho_{S_1^{(1)} S_a} \right. \\
&- \mathcal{G}_{S_1^{(0)} S_2^{(0)}, S_1^{(3)} S_c}^r(\Omega_3 + \omega_4) \mathcal{G}_{S_2^{(3)} S_c, S_2^{(2)} S_b}^r(T_2) \mathcal{G}_{S_1^{(2)} S_b, S_1^{(1)} S_a}^r(\Omega_1 + \omega_1) \rho_{S_a S_2^{(1)}} \\
&+ \mathcal{G}_{S_1^{(0)} S_2^{(0)}, S_1^{(3)} S_c}^r(\Omega_3 + \omega_4) \mathcal{G}_{S_2^{(3)} S_c, S_2^{(2)} S_b}^r(T_2) \mathcal{G}_{S_1^{(2)} S_b, S_a S_2^{(1)}}^r(\Omega_1 + \omega_1) \rho_{S_1^{(1)} S_a} \\
&- \mathcal{G}_{S_1^{(0)} S_2^{(0)}, S_c S_2^{(3)}}^r(\Omega_3 + \omega_4) \mathcal{G}_{S_c S_1^{(3)}, S_b S_1^{(2)}}^r(T_2) \mathcal{G}_{S_b S_2^{(2)}, S_1^{(1)} S_a}^r(\Omega_1 + \omega_1) \rho_{S_a S_2^{(1)}} \\
&+ \mathcal{G}_{S_1^{(0)} S_2^{(0)}, S_c S_2^{(3)}}^r(\Omega_3 + \omega_4) \mathcal{G}_{S_c S_1^{(3)}, S_2^{(2)} S_b}^r(T_2) \mathcal{G}_{S_1^{(2)} S_b, S_1^{(1)} S_a}^r(\Omega_1 + \omega_1) \rho_{S_a S_2^{(1)}} \\
&- \mathcal{G}_{S_1^{(0)} S_2^{(0)}, S_1^{(3)} S_c}^r(\Omega_3 + \omega_4) \mathcal{G}_{S_2^{(3)} S_c, S_b S_1^{(2)}}^r(T_2) \mathcal{G}_{S_b S_2^{(2)}, S_a S_2^{(1)}}^r(\Omega_1 + \omega_1) \rho_{S_1^{(1)} S_a} \\
&+ \mathcal{G}_{S_1^{(0)} S_2^{(0)}, S_1^{(3)} S_c}^r(\Omega_3 + \omega_4) \mathcal{G}_{S_2^{(3)} S_c, S_b S_1^{(2)}}^r(T_2) \mathcal{G}_{S_b S_2^{(2)}, S_1^{(1)} S_a}^r(\Omega_1 + \omega_1) \rho_{S_a S_2^{(1)}} \\
&\left. - \mathcal{G}_{S_1^{(0)} S_2^{(0)}, S_c S_2^{(3)}}^r(\Omega_3 + \omega_4) \mathcal{G}_{S_c S_1^{(3)}, S_2^{(2)} S_b}^r(T_2) \mathcal{G}_{S_1^{(2)} S_b, S_a S_2^{(1)}}^r(\Omega_1 + \omega_1) \rho_{S_1^{(1)} S_a} \right)
\end{aligned} \tag{A1}$$

Here ρ_{ab} is the reduced density matrix,

$$\mathcal{G}_{ab,cd}^r(t) \equiv -i\theta(t) \ll ba | e^{-i\mathcal{L}t} | dc \gg \tag{A2}$$

is the Liouville space retarded Green function [71], and \mathcal{L} is the Liouvillian. Fourier transform of the retarded Green function is

$$\mathcal{G}_{ab,cd}^r(E) = \sum_\gamma \frac{\ll ba | R_\gamma \gg \ll L_\gamma | dc \gg}{E - \lambda_\gamma + i\delta} \tag{A3}$$

where $\delta \rightarrow 0^+$ and λ_γ , $|R_\gamma \gg$ and $\ll L_\gamma|$ are eigenvalues and right and left eigenvectors of the Liouvillian, respectively

$$\mathcal{L} = \sum_\gamma |R_\gamma \gg \lambda_\gamma \ll L_\gamma| \tag{A4}$$

Appendix B: NEGF expression for stimulated signal

For the quadratic (non-interacting) model of Fig. 4 multi-time correlation functions in Eq.(13) can be evaluated employing the Wick's theorem [72]. This leads to exact expression for stimulated signal

$$\begin{aligned}
S_{stim}(\Omega_1, T_2, \Omega_3) &\equiv \int_0^\infty dT_3 \int_0^\infty dT_1 e^{i\Omega_3 T_3 + i\Omega_1 T_1} S_{stim}(T_3, T_2, T_1) = 2 \text{Re} \sum_{\substack{m_0, m_1 \\ m_2, m_3 = \{1,2\}}} E_4^* E_3 E_2^* E_1 e^{i\phi} \\
&\mu_{m_0 3} \mu_{3 m_1} \mu_{m_2 3} \mu_{3 m_3} 2\pi \delta(\omega_1 - \omega_2 + \omega_3 - \omega_4) \int_{-\infty}^{+\infty} \frac{d\epsilon_1}{2\pi} \int_{-\infty}^{+\infty} \frac{d\epsilon_2}{2\pi} e^{iT_2(\omega_1 - \omega_2 + \epsilon_1 - \epsilon_2)} \\
&\left(\left[G_{m_1 m_2}^<(\epsilon_2 - \omega_1 - \omega_1) G_{33}^>(\epsilon_2) - G_{m_1 m_2}^>(\epsilon_2 - \Omega_1 - \omega_1) G_{33}^<(\epsilon_2) \right] A_{m_3 m_0}(\epsilon_2 - \Omega_3 - \omega_4) A_{33}(\epsilon_1) \right. \\
&\left. + \left[G_{m_1 m_0}^<(\epsilon_1) G_{33}^>(\epsilon_1 + \Omega_1 + \omega_1) - G_{m_1 m_0}^>(\epsilon_1) G_{33}^<(\epsilon_1 + \Omega_1 + \omega_1) \right] A_{m_3 m_2}(\epsilon_2) A_{33}(\epsilon_1 + \Omega_3 + \omega_4) \right) \tag{B1}
\end{aligned}$$

Here $G_{m_1 m_2}^{<(>)}(E)$ is Fourier transform of the lesser (greater) projection of the (dashed) particle Green function spectral function.
 $G_{m_1 m_2}(\tau_1, \tau_2) \equiv -i \langle T_c \hat{d}_{m_1}(\tau_1) \hat{d}_{m_2}^\dagger(\tau_2) \rangle$ \tag{B2}

-
- [1] P. Tian, D. Keusters, Y. Suzuki, and W. S. Warren, *Science* **300**, 1553 (2003).
- [2] A. Abboto, L. Beverina, S. Bradamante, A. Facchetti, C. Klein, G. A. Pagani, M. Redi-Abshiro, and R. u. Wortmann, *Chemistry A European Journal* **9**, 1991 (2003).
- [3] T. Brixner, T. Manal, I. V. Stiopkin, and G. R. Fleming, *The Journal of Chemical Physics* **121**, 4221 (2004).
- [4] P. Fischer and F. Hache, *Chirality* **17**, 421 (2005).
- [5] Z. S. Yoon, J. H. Kwon, M.-C. Yoon, M. K. Koh, S. B. Noh, J. L. Sessler, J. T. Lee, D. Seidel, A. Aguilar, S. Shimizu, M. Suzuki, A. Osuka, and D. Kim, *J. Am. Chem. Soc.* **128**, 14128 (2006).
- [6] D. Zigmantas, E. L. Read, T. Manal, T. Brixner, A. T. Gardiner, R. J. Cogdell, and G. R. Fleming, *Proc. Natl. Acad. Sci.* **103**, 12672 (2006).
- [7] I. T. G. Goodson, *Acc. Chem. Res.* **38**, 99 (2005).
- [8] W.-L. Chan, M. Ligges, A. Jailaubekov, L. Kaake, L. Miaja-Avila, and X.-Y. Zhu, *Science* **334**, 1541 (2011).
- [9] T. Steinel, J. B. Asbury, S. Corcelli, C. Lawrence, J. Skinner, and M. Fayer, *Chem. Phys. Lett.* **386**, 295 (2004).
- [10] J. R. Schmidt, S. A. Corcelli, and J. L. Skinner, *J. Chem. Phys.* **123**, 044513 (2005).
- [11] T. Fennel, K.-H. Meiwes-Broer, J. Tiggesbäumker, P.-G. Reinhard, P. M. Dinh, and E. Suraud, *Rev. Mod. Phys.* **82**, 1793 (2010).
- [12] M. Shapiro and P. Brumer, *Principles of the Quantum Control of Molecular Processes* (Wiley, New York, 2003).
- [13] D. Goswami, *Phys. Rep.* **374**, 385 (2003).
- [14] Y. Silberberg, *Ann. Rev. Phys. Chem.* **60**, 277 (2009).
- [15] S. C. Davis, B. W. Pogue, R. Springett, C. Leussler, P. Mazurkewitz, S. B. Tuttle, S. L. Gibbs-Strauss, S. S. Jiang, H. Deghani, and K. D. Paulsen, *Review of Scientific Instruments* **79**, 064302 (2008).
- [16] W. Min, C. W. Freudiger, S. Lu, and X. S. Xie, *Ann. Rev. Phys. Chem.* **62**, 507 (2011).
- [17] S. Mukamel, *Principles of Nonlinear Optical Spectroscopy* (Oxford University Press, 1995).
- [18] V. M. Axt and S. Mukamel, *Rev. Mod. Phys.* **70**, 145 (1998).
- [19] F. C. Spano and S. Mukamel, *Phys. Rev. A* **40**, 5783 (1989).
- [20] K. Okumura and Y. Tanimura, *J. Chem. Phys.* **106**, 1687 (1997).
- [21] K. Okumura and Y. Tanimura, *J. Chem. Phys.* **107**, 2267 (1997).
- [22] A. Tokmakoff, *J. Phys. Chem. A* **104**, 4247 (2000).
- [23] M. Ovchinnikov, V. A. Apkarian, and G. A. Voth, *J. Chem. Phys.* **114**, 7130 (2001).
- [24] Q.-H. Xu, , and G. R. Fleming, *J. Phys. Chem. A* **105**, 10187 (2001).
- [25] T. Renger, V. May, and O. Khn, *Phys. Rep.* **343**, 137 (2001).
- [26] K. Okumura and Y. Tanimura, *J. Phys. Chem. A* **107**, 8092 (2003).
- [27] S. Mukamel, , and D. Abramavicius, *Chem. Rev.* **104**, 2073 (2004).
- [28] F. Šanda and S. Mukamel, *Phys. Rev. A* **71**, 033807 (2005).
- [29] A. G. Lambert, P. B. Davies, and D. J. Neivandt, *Applied Spectroscopy Reviews* **40**, 103 (2005).
- [30] L. Yang and S. Mukamel, *Phys. Rev. B* **77**, 075335 (2008).
- [31] U. Harbola and S. Mukamel, *Phys. Rev. B* **79**, 085108 (2009).
- [32] Z. Ioffe, T. Shamai, A. Ophir, G. Noy, I. Yutsis, K. Kfir, O. Cheshnovsky, and Y. Selzer, *Nature Nanotech.* **3**, 727 (2008).
- [33] D. R. Ward, N. J. Halas, J. W. Ciszek, J. M. Tour, Y. Wu, P. Nordlander, and D. Natelson, *Nano Lett.* **8**, 919 (2008).
- [34] D. R. Ward, D. A. Corley, J. M. Tour, and D. Natelson, *Nature Nanotech.* **6**, 33 (2011).
- [35] M. Banik, P. Z. El-Khoury, A. Nag, A. Rodriguez-Perez, N. Guarrott-xena, G. C. Bazan, and V. A. Apkarian, *ACS Nano* **6**, 10343 (2012).
- [36] P. Z. El-Khoury, D. Hu, V. A. Apkarian, and W. P. Hess, *Nano Lett.* **13**, 1858 (2013).
- [37] M. Galperin and A. Nitzan, *Phys. Chem. Chem. Phys.* **14**, 9421 (2012).
- [38] Y. Xue, S. Datta, and M. A. Ratner, *Chemical Physics* **281**, 151 (2002).
- [39] M. Brandbyge, J.-L. Mozos, P. Ordejón, J. Taylor, and K. Stokbro, *Phys. Rev. B* **65**, 165401 (2002).
- [40] M. Galperin and A. Nitzan, *J. Chem. Phys.* **124**, 234709 (2006).
- [41] M. Galperin and S. Tretiak, *J. Chem. Phys.* **128**, 124705 (2008).
- [42] M. Galperin, M. A. Ratner, and A. Nitzan, *Nano Lett.* **9**, 758 (2009).
- [43] M. Galperin, M. A. Ratner, and A. Nitzan, *J. Chem. Phys.* **130**, 144109 (2009).
- [44] M. Galperin and A. Nitzan, *J. Phys. Chem. Lett.* **2**, 2110 (2011).
- [45] M. Galperin and A. Nitzan, *Phys. Rev. B* **84**, 195325 (2011).
- [46] T.-H. Park and M. Galperin, *Europhys. Lett.* **95**, 27001 (2011).
- [47] T.-H. Park and M. Galperin, *Phys. Rev. B* **84**, 075447 (2011).
- [48] M. Oren, M. Galperin, and A. Nitzan, *Phys. Rev. B* **85**, 115435 (2012).
- [49] T.-H. Park and M. Galperin, *Phys. Scr. T* **151**, 014038 (2012).
- [50] M. Banik, V. A. Apkarian, T.-H. Park, and M. Galperin, *J. Phys. Chem. Lett.* **4**, 88 (2013).
- [51] S. Dey, M. Banik, E. Hulkko, K. Rodriguez, V. A. Apkarian, M. Galperin, and A. Nitzan, *Phys. Rev. B* **93**, 035411 (2016).
- [52] A. Nitzan, *Chemical Dynamics in Condensed Phases* (Oxford University Press, 2006).
- [53] U. Harbola, B. K. Agarwalla, and S. Mukamel, *J. Chem. Phys.* **141**, 074107 (2014).
- [54] B. K. Agarwalla, U. Harbola, W. Hua, Y. Zhang, and S. Mukamel, *J. Chem. Phys.* **142**, 212445 (2015).
- [55] H.-P. Breuer and F. Petruccione, *The Theory of Open Quantum Systems* (Oxford University Press, 2003).
- [56] A. J. White, M. A. Ochoa, and M. Galperin, *J. Phys. Chem. C* **118**, 11159 (2014).

- [57] A. J. White, S. Tretiak, and M. Galperin, *Nano Lett.* **14**, 699 (2014).
- [58] H. Haug and A.-P. Jauho, *Quantum Kinetics in Transport and Optics of Semiconductors* (Springer, Berlin Heidelberg, 2008).
- [59] For classical field these terms drop out by symmetry in the case of isotropic medium [17].
- [60] C. A. Marx, U. Harbola, and S. Mukamel, *Phys. Rev. A* **77**, 022110 (2008).
- [61] Note that at this point we lose photon induced electron electron interaction.
- [62] M. Eckstein and P. Werner, *Phys. Rev. B* **82**, 115115 (2010).
- [63] J. H. Oh, D. Ahn, and V. Bubanja, *Phys. Rev. B* **83**, 205302 (2011).
- [64] A. J. White and M. Galperin, *Phys. Chem. Chem. Phys.* **14**, 13809 (2012).
- [65] H. Aoki, N. Tsuji, M. Eckstein, M. Kollar, T. Oka, and P. Werner, *Rev. Mod. Phys.* **86**, 779 (2014).
- [66] Note that all states of a optical correlation function are of the same type.
- [67] N. S. Wingreen and Y. Meir, *Phys. Rev. B* **49**, 11040 (1994).
- [68] Y. Selzer and U. Peskin, *J. Phys. Chem. C* **117**, 22369 (2013).
- [69] M. A. Ochoa, Y. Selzer, U. Peskin, and M. Galperin, *J. Phys. Chem. Lett.* **6**, 470 (2015).
- [70] M. Esposito and M. Galperin, *J. Phys. Chem. C* **114**, 20362 (2010).
- [71] M. Esposito and M. Galperin, *Phys. Rev. B* **79**, 205303 (2009).
- [72] A. L. Fetter and J. D. Walecka, *Quantum Theory of Many-Particle Systems* (McGraw-Hill Book Company, 1971).